Determination of the surface recombination velocity of unpassivated silicon from spectral photoconductance measurements

Conference Paper · June 2003

DOI: 10.1109/WCPEC.2003.1305222 · Source: IEEE Xplore

DETERMINATION OF THE SURFACE RECOMBINATION VELOCITY OF UNPASSIVATED SILICON FROM SPECTRAL PHOTOCONDUCTANCE MEASUREMENTS

Helmut Mäckel and Andrés Cuevas
Dept. of Engineering, Faculty of Engineering and Information Technology,
Australian National University, Canberra ACT 0200, Australia.

ABSTRACT

Bare, non-diffused silicon wafers of different resistivities and surface conditions have been analyzed with a spectral photoconductance technique. The surface recombination velocity has been calculated by fitting the measurements with a theoretical model. The main result is that the surface recombination velocity is not constant, but decreases with increased resistivity, both for n-type and p-type wafers. The surface recombination velocity was found to vary from $\sim$10 cm/s for 1000 Ωcm Si to $\sim 10^5$ cm/s for 0.3 Ωcm Si. These values are much lower than the previously assumed 'infinite' surface recombination velocity of 10^6-10^7 cm/s for bare silicon.

1. INTRODUCTION

The surface recombination velocity, S, has a substantial impact on the performance of solar cells. The knowledge of S is particularly important to classify measurements of the effective lifetime. In industrial silicon solar cell fabrication, effective lifetime measurements are used prior to processing to evaluate the quality of the bulk material. In multicrystalline silicon the bulk lifetime can vary with the location inside the ingot from were the wafer has been cut out. The knowledge of S may permit a more accurate determination of the bulk lifetime. The measurement of S of unpassivated silicon can also be used to determine the amount of residual surface damage and optimize its elimination.

In bare silicon, a very high S of 10^6-10^7 cm/s has usually been assumed to calculate the bulk lifetime, independently of the wafer resistivity. We have performed spectral measurements of the photoconductance of bare silicon in order to calculate accurate values for the surface recombination velocity. Our measurements indicate that the actual S is lower than 1.5x10^5 and depends strongly on the doping density of the wafer.

2. THEORY

The external quantum efficiency of the photoconductance is defined in a similar way as the external quantum efficiency of the short-circuit current, $EQE(J_{sc}, \lambda)$ [1, 2]. It is given by the ratio of the excess photoconductance, $\Delta\sigma$, to the incident photon flux on the surface of the sample, N_{ph}:

$$EQE(\Delta\sigma, \lambda) = \frac{\Delta\sigma(\lambda)}{qN_{ph}(\lambda)}. \quad (1)$$

The main physical difference to $EQE(J_{sc}, \lambda)$ is that in the $EQE(\Delta\sigma, \lambda)$ we measure the cumulative excess carrier change in the wafer, while in the $EQE(J_{sc}, \lambda)$ we measure the number of carriers that are detected at the pn-junction.

In the following, we have used an analytical model that describes $EQE(\Delta\sigma, \lambda)$ and includes the surface recombination as a fitting parameter. The derivation starts with the wavelength-dependent continuity equation in low-injection:

$$D_n \frac{d^2\Delta n(x)}{dx^2} + \frac{\Delta n(x)}{\tau_b} - G(\lambda, x) = 0, \quad (2)$$

with D_n: diffusion coefficient, Δn: carrier density, τ_b: bulk lifetime. $G(\lambda, x)$ is a function of the photon flux, the front and back reflectance and the absorption coefficient and can be found e.g. in ref. [3]. To obtain an analytical solution we consider τ_b, μ_n and μ_p independent of the injection level. Nevertheless, a careful selection of the specific values for these parameters permits us to account for their injection level dependence. For a particular excess photoconductance, either measured or simulated, an average value for Δn is obtained through a series of iterations that use injection level dependent mobilities [4], until a self-consistent set of values for Δn_{av} and $\mu_n + \mu_p$ is derived. This value of $\mu_n + \mu_p$ is then used in the theoretical simulations of $EQE(\Delta\sigma, \lambda)$. The bulk lifetime is calculated using a fit of Kerr *et al.*, which accounts for the dependance of τ_b with injection level and doping concentration [5]. The excess photoconductance can then be obtained as:

$$\Delta\sigma \approx q(\mu_n + \mu_p) \int \Delta n dx. \quad (3)$$

In the case of low-injection, the external quantum efficiency of the photoconductance of non-diffused silicon can then be expressed as a function of the surface recombination velocity and the bulk lifetime, using the boundary conditions for the front and back surfaces:

$$EQE(\Delta\sigma, \lambda) = (\mu_n + \mu_p)\, \tau_b\, f_{abs}(\lambda) + (\mu_n + \mu_p)\, f(S_f, S_b, \tau_b, \lambda), \quad (4)$$

where f_{abs} is the absorption fraction and $f(S_f, S_b, \tau_b, \lambda)$ is a function of the front and back surface recombination velocity, the bulk lifetime and the wavelength and will be published elsewhere [6]. The optical parameters of the wafers are modelled by the ray-tracing software Sunrays [7]. In all cases, S_{eff}=S_f=S_b has been assumed, so that S_{eff} remains the only fitting parameter. A least-square procedure has been used to model the measurement with Eq. 4.

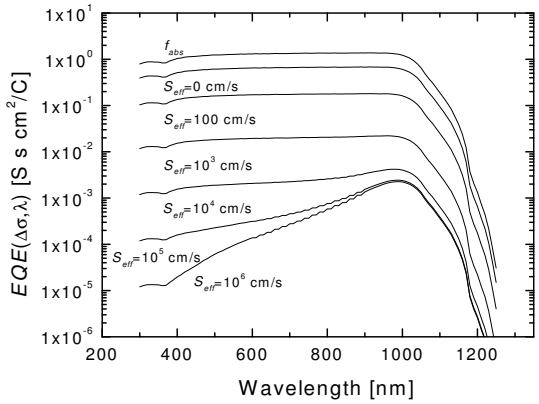

Fig. 1: The external quantum efficiency of the photoconductance and the absorption fraction as a function of wavelength of a unpassivated silicon wafer for different S_{eff}. The parameter used for the calculations are: thickness 300 μm, resistivity 1 Ωcm, fixed electron and hole carrier mobilities of 1520 and 500 cm^{-2}/Vs, respectively and a fixed bulk lifetime of 1000 μs. S_{eff}=S_f=S_b has been varied from 0 to 10^6 cm/s.

In the case of zero surface recombination, the external quantum efficiency is determined by the absorption fraction and the bulk lifetime (Eq. 4). A lower bulk lifetime therefore decreases the external quantum efficiency independently of the wavelength. For high S_{eff} the second term in Eq. 4 leads to a characteristic hump in the long wavelength response. We demonstrate this in Fig. 1 with the simulation of the external quantum efficiency of a non-passivated 1 Ωcm p-type silicon wafer with electron and hole carrier mobilities of 1520 and 500 cm^{-2}/Vs, respectively and a fixed bulk lifetime of 1000 μs. The surface recombination velocity, S_{eff}=S_f=S_b, has been varied from 0 to 10^6 cm/s. Additionally, a typical absorption fraction of a bare silicon wafer is shown in Fig. 1. The external quantum efficiency is significantly lowered by increasing S_{eff}. As S_{eff} increases above 10^4 cm/s, the hump becomes clearly visible. This is due to the fact that the finite diffusion coefficient D_n limits the flow of carriers generated deep in the wafer towards the surfaces [1]. A similar effect has been seen in studies of the external quantum efficiency of the photoconductance of emitter samples [1, 2]. It should be mentioned that the analytical model agrees perfectly with PC1D simulations and that the shape of the external quantum efficiency is only slightly affected in the IR if S_b is changed.

3. EXPERIMENTAL

A range of polished, as-cut and lapped p-type and n-type FZ silicon wafers with resistivities between 0.3 and 1000 Ωcm have been used for the investigation. Table 1 specifies the characteristics of the wafers.

Table 1: Characteristics of the non-passivated wafers used in this investigation. The orientation was <100> apart from the 7 Ωcm wafer, where the orientation is not known.

Surface condition	Resistivity [Ωcm]	Type	Growth	Thickness [μm]
polished	0.3	p	FZ	305
polished	0.5	p	FZ	400
polished	1	p	FZ	295
polished	2	n	FZ	480
polished	4.5	p	FZ	300
polished	7	n	FZ	380
polished	10	n	CZ	450
polished	50	p	FZ	295
polished	100	n	FZ	290
polished	1000	n	FZ	285
as cut	0.5	p	FZ	420
as cut	1	p	FZ	570
as cut	1.75	n	FZ	360
as cut	145	p	FZ	525
lapped	20	n	FZ	240
lapped	88	n	FZ	315

The quasi-steady-state excess photoconductance of the wafers has been measured with a contactless inductively coupled photoconductance apparatus [8]. Bandpass filters with a bandwidth of 10 nm have been used to produce monochromatic light. The illumination produces an excess photoconductance, $\Delta\sigma$, over the equilibrium conductivity of the material, which is proportional to the average excess carrier concentration, Δn_{av}. Due to the dependence of recombination on the carrier density, measurements made at different wavelengths have been performed at the same injection level to ensure comparability. Practically this can be achieved by comparing all measurements at the same excess photoconductance [1].

4. RESULTS AND DISCUSSION

Fig. 2 shows the comparison of measured and simulated $EQE(\Delta\sigma, \lambda)$. The simulated $EQE(\Delta\sigma, \lambda)$ of the 100 Ωcm n-type wafer is characterized by a flat response. In contrast, the measurement shows a hump in the IR. In this case, the measurement is not well described by the simple analytical formula developed in section 2. Fortunately, this problem only occurs for high resistivity wafers (>50 Ωcm) with low spectral response. As can be seen in the second example in Fig. 2, the external spectral response of the 2 Ωcm n-type wafer can be fitted excellently. At present, neither the analytical model nor PC1D can explain the phenomenon in high resistivity wafers; it is possible

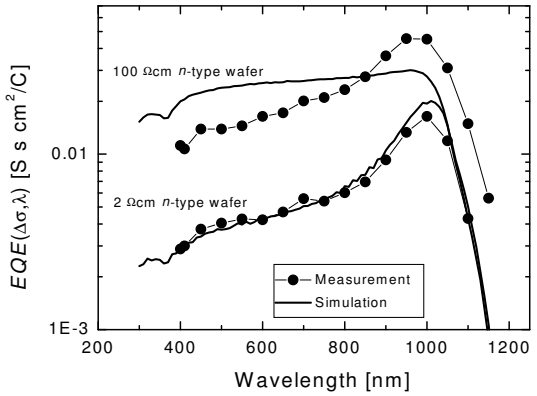

Fig. 2: Measurement and simulation of ESR as a function of wavelength for two cases: a 100 Ωcm n-type and a 2 Ωcm n-type wafer. In the first case, ESR can not be fitted accurately, while the second fit is in excellent agreement with the measurement.

that the assumption of a constant mobility is inappropriate in this case. In the following, S_{eff} values where the simulation matched the measurement only inaccurately are shown in brackets.

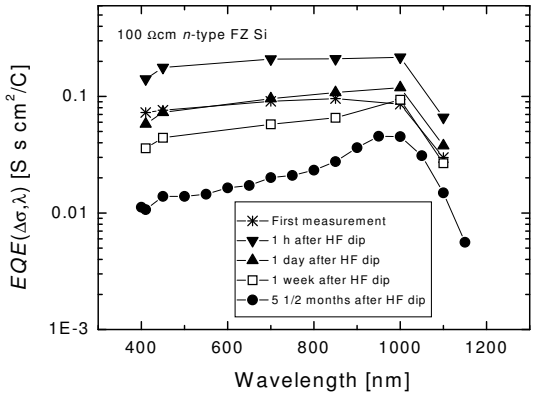

Fig. 3: Evolution of the external spectral response of the excess photoconductance of a polished 100 Ωcm n-type wafer after HF dip and with time.

We noticed that the external quantum efficiency of the photoconductance of polished bare silicon is very sensitive to surface treatment. This is illustrated in Fig. 3 with the evolution of $EQE(\Delta\sigma, \lambda)$ of a 100 Ωcm n-type wafer before and after a HF dip and with storage time. The sample was: 1) taken 'out of the box' and measured, 2) cleaned in a 5% HF solution, rinsed in DI water and measured 1 h after the dip, 3) measured 1 day, 1 week and 5 1/2 months after the rinse. After the HF dip, the external quantum efficiency increased strongly, but decreased again with time until it regained the same magnitude after 1 week. Unexpectedly, the external quantum efficiency decreased further after 5 1/2 months. The changes of the fitted S_{eff} due to the HF dip and the subsequent storage for several polished n and p-type wafers are shown in Fig. 4. It illustrates that this phenomenon is common for all wafer resistivities, but slightly stronger for low resistivities. The range of S_{eff} between the HF treatment and several months after the treatment spans 1-2 orders of magnitudes. We obtain an excellent S_{eff} of 5.8 cm/s for the 1000 Ωcm n-type wafer after HF dip. The highest S_{eff} in the graph is 1.3×10^5 cm/s for the 1 Ωcm p-type wafer after 5 1/2 months.

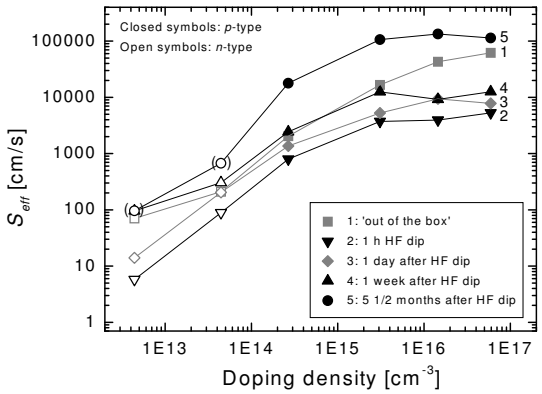

Fig. 4: Evolution of S_{eff} of polished Si wafers of different resistivities after an HF dip and with time. Values in brackets indicate that theses measurements can not be modelled accurately.

It is well known that an immersion in hydrofluoric acid serves as an excellent passivation of silicon, comparable to that of SiO_2/Si interfaces [9]. In general, best results have been produced, if the surface has been oxidised prior to the HF dip. The HF treatment leads to a positive surface charge causing a strong inversion in p-type Si and an accumulation in n-type Si independent of the time of the HF dip [10]. After the HF treatment, the electronic properties are stable for up to 300 min [10]. The growth of the first monolayer coverage of native oxide takes between 2 hours [11] and 7 days [12]. In this period the electronic properties change strongly, particularly the positive surface charge and the density of extrinsic states reduces. The oxidation stabilizes after 70-700 days [11, 12] and the electric properties become similar to the thermally oxidized Si/SiO_2 interface but generally with a higher density of states [10].

These observations help to explain the changes in $EQE(\Delta\sigma, \lambda)$ in our wafers. The surface conditions of the polished wafers taken 'out of the box' are not clear. Most likely, they have a thin oxide on the surface, probably created by chemical cleaning after wafer polishing. The flat curve of $EQE(\Delta\sigma, \lambda)$ (Fig. 3) for the 'out of the box' condition indicates a relatively well passivated surface. The dissolution of the oxide layer in hydrofluoric acid initially produces an even better passivation due to an almost ideal hydrogen termination of Si dangling bonds [9, 13] and a higher fixed positive charge. After exposure to air, the wafers traverse a phase of rapidly changing electronic properties at the surface, which is manifested by the decrease of the spectral response. After 5 1/2 months the native oxide stabilized, yet to a different state than the wafers 'out of the box'. The last measurement of $EQE(\Delta\sigma, \lambda)$ in (Fig. 3) represents therefore the stable state of a polished Si wafer covered with a native oxide.

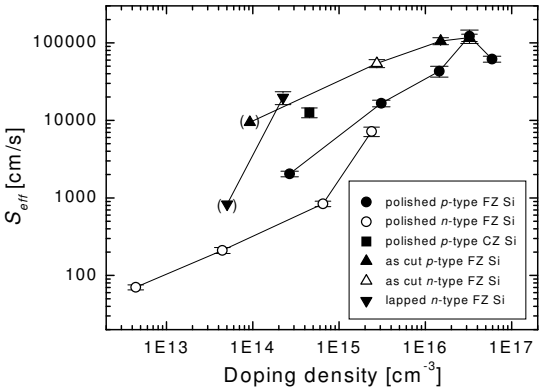

Fig. 5: S_{eff} of bare silicon wafers of different material and surface conditions taken 'out of the box'. The error bars are calculated from an assumed measurement error of ESR of 10% and from a variation of S_{eff} due to the injection dependence of ESR. Only for the 100 and 1000 Ωcm n-type wafer this variation in S_{eff} was bigger than the measurement error. Values in brackets indicate that theses measurements can not be modelled accurately.

Finally, we turn our focus to the determination of S_{eff} of as-cut and lapped wafers taken 'out of the box' (Fig. 5). Included in Fig. 5 are as well the measurements of polished wafers in the 'out of the box' condition. S_{eff} shows a tendency to increase with increasing doping concentration. In general, the as cut and lapped wafers show a higher S_{eff} than the polished wafers. For the latter, n-type wafers seem to exhibit better surface recombination than their p-type counterparts. The values of S_{eff} range from 70 cm/s for 1000 Ωcm Si to 1.2x10^5 cm/s for 0.5 Ωcm Si and are much lower as the previously assumed surface recombination velocity of 10^6-10^7 cm/s for bare silicon.

5. CONCLUSIONS

The measured external spectral response of the excess photoconductance can be accurately simulated by the analytical model proposed in this investigation for low resistivity wafers. For high resistivities and low spectral response, a hump in the IR which is not predicted by the theory impedes the accurate extraction of S_{eff}. Neither the analytical model nor PC1d calculation are able to clarify this problem. The S_{eff} generally increases with increasing doping density and is higher for as cut and lapped wafers than for polished wafers taken 'out of the box'. The investigation indicates that polished n-type wafer show a higher surface quality than p-type wafers for a given doping density.

The external spectral response of the excess photoconductance of polished wafers is subject of dramatic changes after a HF treatment. Changes in the fixed positive oxide charges and in the density of states of the SiO_2/Si interface are likely the reason for this effect. Due to this change, S_{eff} can vary 1-2 orders of magnitude depending on surface treatment. Thus, the surface conditions has to be taken in account before assuming S_{eff} of bare silicon in experiments or simulations.

6. ACKNOWLEDGEMENTS

Helmut Mäckel has been supported by a scholarship of the P.h.D. program of the Deutsche Akademische Austausch Dienst (DAAD). This project has been funded by a grant of the Australian Research Council (ARC).

REFERENCES

[1] A. Cuevas, R.A. Sinton, M. Kerr, D.H. Macdonald and H. Mäckel, Solar Energy Material and Solar Cells **71**, 295 (2002).

[2] H. Mäckel, A. Cuevas and W. Warta, *ISES 2001 Solar World Congress*, Adelaide, South Australia, to be published.

[3] M. Bail and R. Brendel, *16th European Photovoltaic Solar energy Conversion*, p. 98, Glasgow, UK, 2000.

[4] P.P. Altermatt, J. Schmidt, M. Kerr, G. Heiser and A.G. Aberle, *16th European Photovoltaics Solar Energy Conference*, p. 243-246, Glasgow, UK, 2000.

[5] M.J. Kerr and A. Cuevas, Journal of Applied Physics **91**, 2473 (2002).

[6] H. Mäckel and A. Cuevas, to be published.

[7] R. Brendel, *Proceedings of the 14th European Photovoltaic Solar Energy Conference*, p. 1339-42, Amsterdam, The Netherlands, 1994.

[8] G.C.S. Consulting, Boulder, CO 80305, USA.

[9] E. Yablonovitch, D.L. Allara, C.C. Chang, T. Gmitter and T.B. Bright, Physical Review Letters **57**, 249 (1986).

[10] T. Dittrich, H. Angermann, W. Fussel and H. Flietner, Physica Status Solidi A **140**, 463 (1993).

[11] M. Morita, T. Ohmi, E. Hasegawa, M. Kawakami and K. Suma, Applied Physics Letters **55**, 562 (1989).

[12] D. Gräf, M. Grundner, R. Schulz and L. Muhlhoff, Journal of Applied Physics **68**, 5155 (1990).

[13] V.A. Burrows, Y.J. Chabal, G.S. Higashi, K. Raghavachari and S.B. Christman, Applied Physics Letters **53**, 998 (1988).